Proceedings of the ASME 2009 International Mechanical Engineering Congress & Exposition
IMECE2009
November 13-19, Lake Buena Vista, Florida, USA

IMECE2009-12513

INVESTIGATION OF INDOOR ENVIRONMENT FOR A DATA CENTER

Lingcang Li[1], Yanlei Liu[1], Xiuling Wang[1] and A. G. Agwu Nnanna[1]

[1]Purdue University Calumet

ABSTRACT

Special indoor air environment requirements are needed for the data center, such as ambient temperature, airflow pattern, relative humidity and ozone concentration to maintain the reliability of a computer system. In this paper, a numerical simulation based on 3-D Finite Volume Method has been conducted for a data center at Purdue University Calumet. The purpose of the simulation is to find out the most effective and low-cost air condition system. Results for temperature, relative humidity distributions as well as velocity patterns are presented. Mesh independent studies are performed. Numerical results are validated by experimental data. Suggestions are given based on the simulation results for improving the indoor environment of the data center.

INTRODUCTION

The reliability of a computer system is dependent upon a stable indoor air environment. The design of the environmental control system for the data center must ensure that each system can operate reliably and satisfy its operating specifications. In the data center at Purdue University Calumet, the under-floor air distribution (UFAD) system is installed. Under-floor air distribution systems have recently become popular design alternatives to conventional air distribution designs such as ceiling air distribution (CAD) systems for ventilation and thermal control [1]. It is predicted by industry-watchers that 35 percent of future office buildings will include UFAD systems because of their potential advantages in reducing cost, space, and improving indoor air quality. Unlike the classical type system - CAD systems-the diffuser of UFAD systems gives a higher air speed at the floor level rather than the ceiling of the room [2]. This kind of air delivery will have great impact on the room air distribution, temperature profile, and contaminant distribution [3].

In order to design and redesign the efficient UFAD systems and to improve the air quality for the data center, we can choose an experimental method. Experimental measurements can only provide information at certain locations in the room and will cost more. Alternatively, numerical modeling and simulation is a low-cost and effective method for the HVAC systems in the design and improvement phase [4]. A detailed evaluation of air flow, heat transfer, and relative humidity in the data center will be provide valuable information in design and redesign the air distribution system for the data center.

The objective of this study is to use numerical modeling to simulate airflow in the data center with a UFAD system in PUC, provide suggestions for constructing an optimized indoor environment for the data center. The commercial software Gambit™ and Fluent™, are used for this purpose. The results can be related to the thermal environment, indoor air quality, and ventilation effectiveness. Temperature and relative humidity (RH) distributions as well as velocity patterns are presented.

NOMENCLATURE

All the nomenclature is shown in non-dimensional form.

c_p	Specific heat of air, J/ (kg·K)
D	Mass diffusivity of species in air, m^2/s
g	Gravitational acceleration, m/s^2
k	Thermal conductivity of air, W/ (m·K)
m	Concentration of species, kg of species
p	Pressure; partial pressure (with subscript), Pa
q	Heat flux, W/m^2
T	Temperature (with subscript), K

u	Velocity, m/s
β	Thermal expansion coefficient, 1/K
φ	Relative humidity
μ	Viscosity of air, kg/ (m·s)
ρ	Density of air, kg/m^3

Subscripts

ref	Reference
s	Saturated (water vapor)
w	Water vapor
x	Component in x-direction (velocity), m/s

GOVERNING EQUATIONS

Consider a steady state and incompressible flow of air as a fluid which includes dry air and water vapor. The fluid properties are considered as constants except for the varying density for buoyancy term in the momentum equation.

The equation of conservation of mass is given by:

$$\nabla u = 0 \qquad (1)$$

And assuming there is no chemical interaction, the equations of conservation of mass for water vapor is listed as follows:

$$u\nabla m_1 = D_1\nabla^2 m_1 \qquad (2)$$

The buoyancy force term arising from density variation is included by means of the Boussinesq approximation based on the assumptions that variation in fluid density affect only the buoyancy term and that the fluid density is a function of temperature and concentration only [5].

The generation of turbulence due to buoyancy is given by:

$$G_b = \beta g_i \frac{\mu_t}{Pr_t}\frac{\partial T}{\partial x_i} \qquad (3)$$

where $Pr_t$is the turbulent Prandtl number for energy and g_i is the component of the gravitational vector in the *i*th direction. For the standard and realizable k-ε models, the default value of Pr_t is 0.85. In the case of the RNG k-ε model, Pr_t=1/α, where α is given by:

$$\left|\frac{\alpha-1.3929}{\alpha_0-1.3929}\right|^{0.6321}\left|\frac{\alpha+2.3929}{\alpha_0+2.3929}\right|^{0.3679} = \frac{\mu_{mol}}{\mu_{eff}} \qquad (4)$$

where $\alpha_0 = 1.0$. In the high-Reynolds-number limit $(\mu_{mol}/\mu_{eff} \ll 1)$. $\alpha_k = \alpha_\varepsilon \approx 1.393$

The coefficient of thermal expansion, β is defined as:

$$\beta = -\frac{1}{\rho}\left(\frac{\partial\rho}{\partial T}\right)_p \qquad (5)$$

The equation of the conservation of momentum is listed as follows:

$$\rho u\nabla u = -\nabla p + \mu\nabla^2 u + \rho g\beta(T - T_{ref}) \qquad (6)$$

The RNG k- ε model was derived using a rigorous statistical technique (called renormalization group theory). It is similar in form to the standard k-ε model, but includes the following refinements:

- The RNG model has an additional term in its ε equation that significantly improves the accuracy for rapidly strained flows.
- The effect of swirl on turbulence is included in the RNG model, enhancing accuracy for swirling flows.
- The RNG theory provides an analytical formula for turbulent Prandtl numbers, while the standard k-ε model uses user-specified, constant values.
- While the standard k-ε model is a high-Reynolds-number model, the RNG theory provides an analytically-derived differential formula for effective viscosity that accounts for low-Reynolds-number effects. Effective use of this feature does, however, depend on an appropriate treatment of the near-wall region.

The RNG model may be written in a form which is similar to the standard k–ε model and it relates the Reynolds stress tensor τ^{ij} to the mean fluid velocity in the following form:

$$\tau^{ij} = -\frac{2}{3}\rho k\delta_j^i + \mu_t\left(\frac{\partial u^i}{\partial x^j} + \frac{\partial u^j}{\partial x^i}\right) \qquad (7)$$

where the turbulent viscosity may be expressed as a function of the turbulent kinetic energy k and its rate of dissipation e as follows:

$$\mu_t = c_\mu\rho\frac{k^2}{\varepsilon} \qquad (8)$$

where c_μ is a constant and it has been found that the value of c_μ = 0:0845 gives good results for a number of investigations, and therefore it has been assigned this value in all the computation presented in this paper.

The equation of conservation of energy is listed as follows:

$$\rho C_p u\nabla T = k\nabla^2 T \qquad (9)$$

Turbulent kinetic energy equation:

$$\rho u^j\frac{\partial k}{\partial x^j} = \alpha\frac{\partial}{\partial x^i}\left((\mu + \mu_t)\frac{\partial\varepsilon}{\partial x^i}\right) + P - \rho\varepsilon \qquad (10)$$

where

$$P = (\mu + \mu_t)\left(\frac{\partial u^i}{\partial x^j} + \frac{\partial u^j}{\partial x^i}\right)\frac{\partial u^i}{\partial x^j} \qquad (11)$$

is the term which represents the production of turbulence.

The relative humidity can be computed by using the procedure recommended by ASHRAE [8], which is summarized as follows:

$$\emptyset = \frac{P_w}{P_{ws}} \quad (12)$$

$$P_w = \frac{(101325+P)m_1}{0.62198+0.37802m_1} \quad (13)$$

$$P_{ws} = \exp\left[-\frac{5.8002206\times10^3}{T_K} + 1.3914993 - 4.8640239\times10^{-2}T_K + 4.1764768\times10^{-5}T_K^2 - 1.4452093\times10^{-8}T_K^3 + 6.549673\ln(T_K)\right] \quad (14)$$

NUMERICAL EXAMPLES

Modeling geometry

The data center experiments were carried out in a full-scale indoor environmental chamber (23.38m×13.11m×3.03 m) as shown in Fig. 1. The configuration represents a chamber with displacement ventilation in the UFAD system. The box-shaped simulators (2.44m×1.22m×2.03 m) represented computers. Air temperatures and velocities were collected at four different poles within the chamber. Each pole had four temperature sampling points, positioned at different heights. Fig. 2 shows the locations for both point sources and measurement poles. Air temperature and velocity data were collected under steady-state conditions. These data were used for the benchmark validation of numerical simulations.

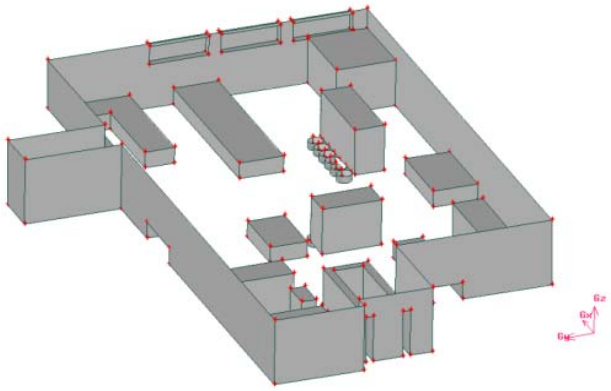

Figure1. Configuration and furniture layout for the data center chamber

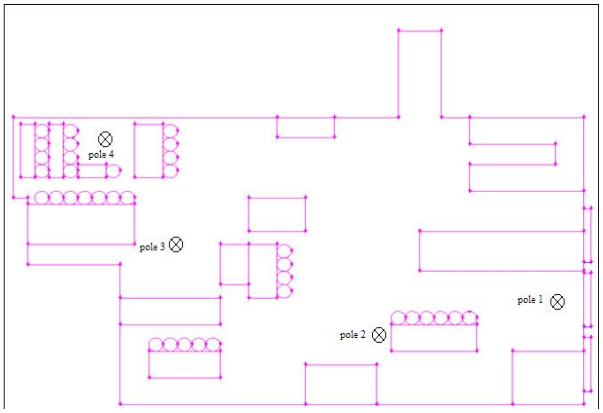

Figure2. Temperature point source and measurement pole locations

Problem definition

Compared to the indoor environment size, the element with artificially enlarged area in simulations can still be considered small enough to represent a point source. Although the element area enlargement is numerically beneficial, its influence on simulation accuracy needs to be determined. In this work, numerical tests were designed to study the influence of element area enlargement on CFD simulations for indoor temperature point sources.

In each element, velocity components and temperature were approximated by using the Galerkin procedure, which led to a set of algebraic equations that defined the discredited continuum. Four-node quadrilateral elements were used. The distribution of the element size in the computational domain was determined from a series of tests with different numbers of elements in the x-, y-and z- directions and for different mesh density around inlet, outlet, and objects where high rates of momentum, heat, and mass transfer exist. By systematically increasing the number of elements as well as the grading ratios and monitoring the residual distribution for all variables in the computational domain, the mesh needed for accurate computation was determined. Mesh independent study was performed. Different numbers of elements were tested: 612,522 elements, 1,225,000 elements and 2,451,200 elements. Based on the comparison of the results, it was found that approximately 1,225,000 elements were needed. Below are some details for the model settings:

i. Considering the turbulent effect, we choose to use the k-e model to solve the indoor air quality simulation [6]

ii. There is no chemical reaction, and radiation is negligible because of the small temperature difference in indoor simulation.

iii. Boundary condition:

   a) Prescribed velocity for inlet, zero velocity for solid surfaces.
   b) Constant temperature condition was used for inlet,

constant heat flux for heated surfaces of lights and computer hot surface, and insulated (no heat flux) for floor and ceiling.

c) We set other conditions as zero mass flux at other solid surfaces and wall [7].

Details of boundary conditions are given in Table 1. The constant fluid properties were taken at reference temperature.

as follows: T_{ref} = 65°F = 18.33°C = 291.49K,
$\rho = 1.1967\ [kg/m^3]$,
$\mu = 1.8273\times10^{-5}\ [kg/(m\cdot s)]$,
$c_p = 1.0043\times10^{-3}\ [J/(kg\cdot K)]$,
$k = 2.5776\times10^{-2}\ [W/(m\cdot K)]$,
$\beta = 3.3932\times10^{-3}\ [K^{-1}]$.

Entity	Mass flow rate	Temperature
Inlet	12.2kg/s	T= 288K
Hot surface	0	(*)
Lightings	0	q= 75W/m^2
Floor	0	(×)
Outlet	(×)	(×)
Others	0	0
(×) *Unknown, to be found as part of numerical solution* (*) *See Table 2 for detailed values*		

Table 1 Boundary conditions

The heat flux rate of each racks are measured from several place. The average value is based on the previous data.

Number	Heat flux rate
Rack 1	109.23W/m^2
Rack 2	80.22W/m^2
Rack 3	115.59W/m^2
Rack 4	101.64W/m^2
Rack 5	80.06W/m^2
Rack 6	98.43W/m^2

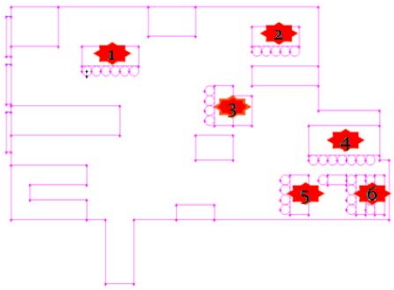

Table 2 Boundary conditions – Hot Surface

Simulation results

1. Velocity

Consider the solution of the typical case (simulation 1). Figure 3 and 4 present the contour of the velocity field and velocity vector.

The cool airflow enters the cubicle vertically through a floor-level diffuser at uniform full speed (1.0 m/s). The incoming flow goes vertically straight at first, then slightly bends separately where the racks are located. As the main flow sweeps along the racks' surface and reaches higher height, its speed decreases significantly due to loss of momentum and the buoyancy effect caused by the temperature-dependent density difference between the main flow, composed by cooler air from the diffuser, and the higher temperature surrounding air, which acts downward and tends to slow the main flow down. At about a third of the space height, the main flow air speed reduces to 0.5 m/s. At the a half of the apace height, the air speed continues to drop to 0.3 m/s. The low pressure at the outlet has the effect of accelerating the main flow in the local region. The air surrounding the inlet diffuser, goes up under the influence of the high-speed inlet flow, and then goes down, creating local circulations on both sides of the diffuser.

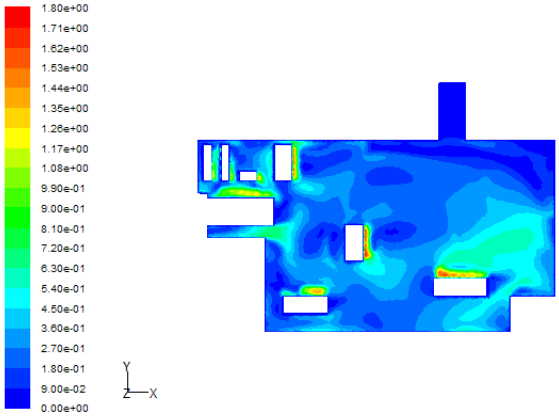

Figure3. Velocity

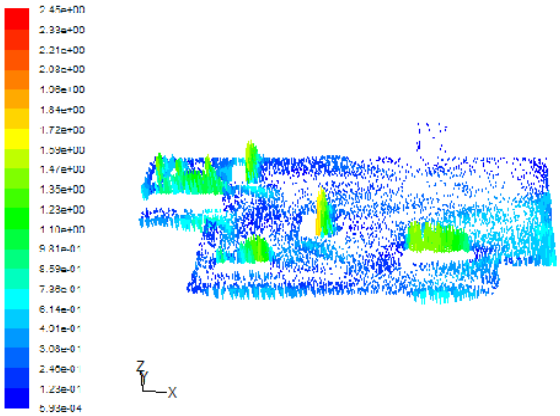

Figure4 Velocity vector

2. Temperature distribution

Figure 5 to 9 show the distributions of temperature in the chamber from different altitudes. They reflect the influences

of the velocity field on the heat transfer phenomenon. Because of their high speed, the main flow keeps its low temperature as 290K all the way from the lowest point to the highest point with very small changes.

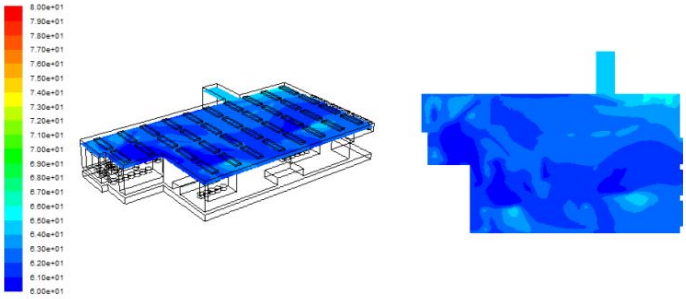

Figure5. Temperature in 3D and 2D (altitude 2.5m)

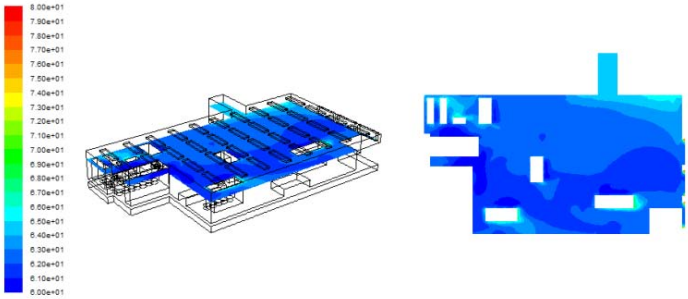

Figure6. Temperature in 3D and 2D (altitude 2.0m)

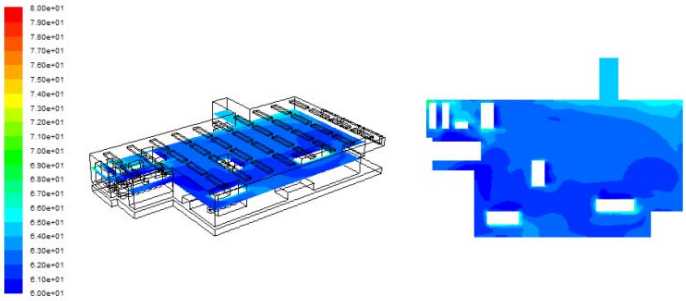

Figure7. Temperature in 3D and 2D (altitude 1.5m)

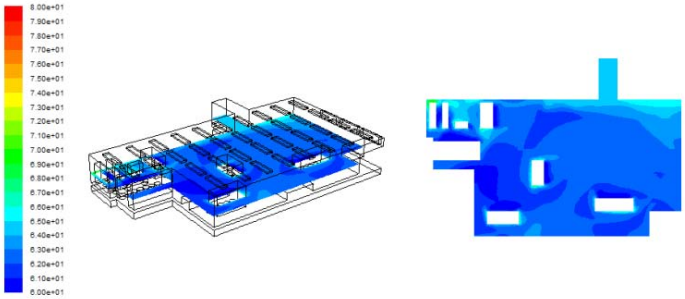

Figure8. Temperature in 3D and 2D (altitude 1.0m)

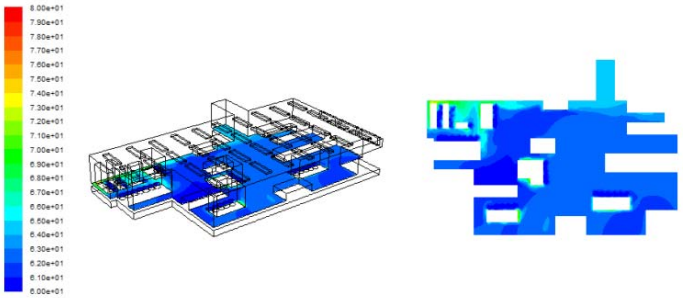

Figure9. Temperature in 3D and 2D (altitude 0.0m)

3. Relative humidity

Figure 10-14 show the distributions of relative humidity in the chamber from different altitudes. They reflect the influences of water vapor concentration on the heat transfer phenomenon. Some areas in the floor level are considered to be the danger area, which the relative humidity of these areas is much lower than the average value.

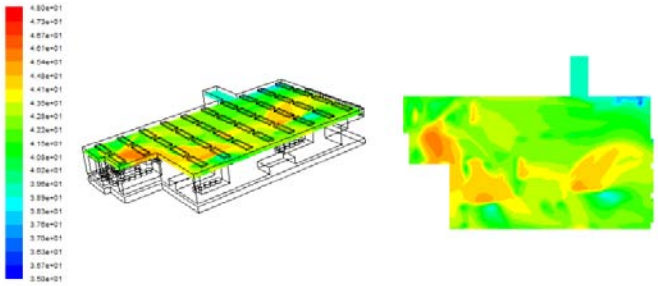

Figure10. Relative humidity in 3D and 2D (altitude 2.5m)

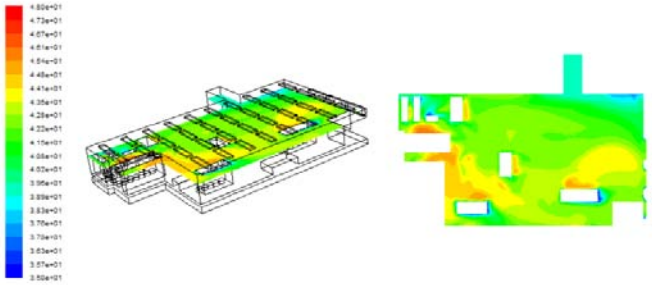

Figure11. Relative humidity in 3D and 2D (altitude 2.0m)

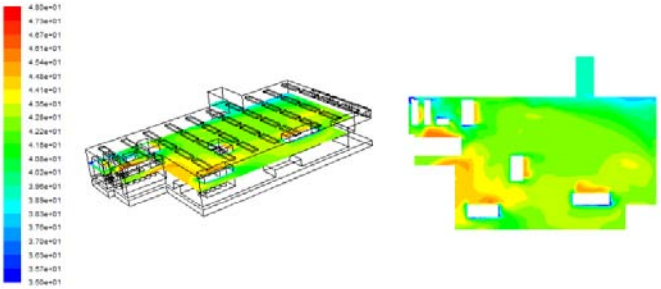

Figure12. Relative humidity in 3D and 2D (altitude 1.5m)

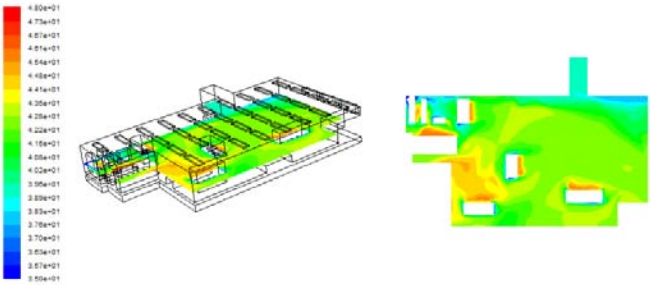

Figure13. Relative humidity in 3D and 2D (altitude 1.0m)

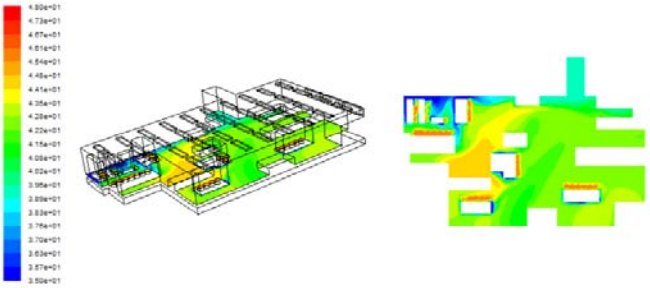

Figure14. Relative humidity in 3D and 2D (altitude 0.0m)

Validation and verification

To further evaluate the accuracy of simulations, the most reliable way is to compare numerical results with experimental data. The comparisons of numerical and experimental data for pole 1, 2, 3 and 4 are shown in Figs. 15-18. For pole 1 and 3, the numerical results are consistent with the experimental data. For pole 2 and 4, the numerical results of some small areas deviate from the experimental results.

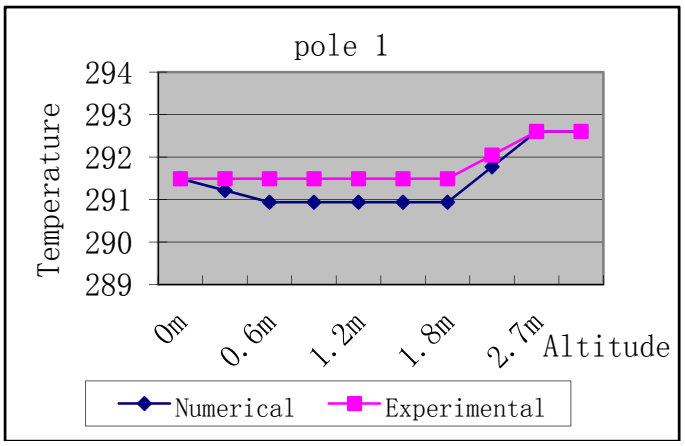

Figure15. Comparison of measured and simulated temperature result on pole 1

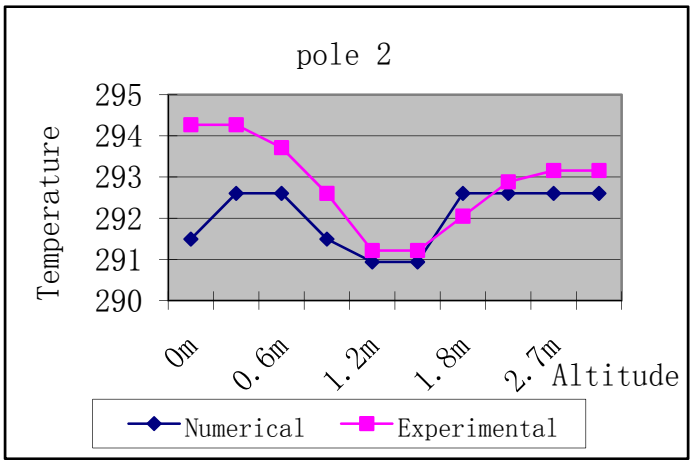

Figure16. Comparison of measured and simulated temperature result on pole 2

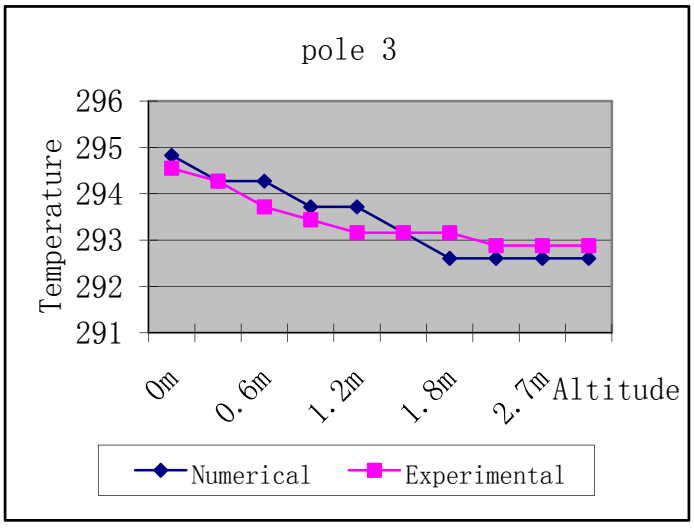

Figure17. Comparison of measured and simulated temperature result on pole 3

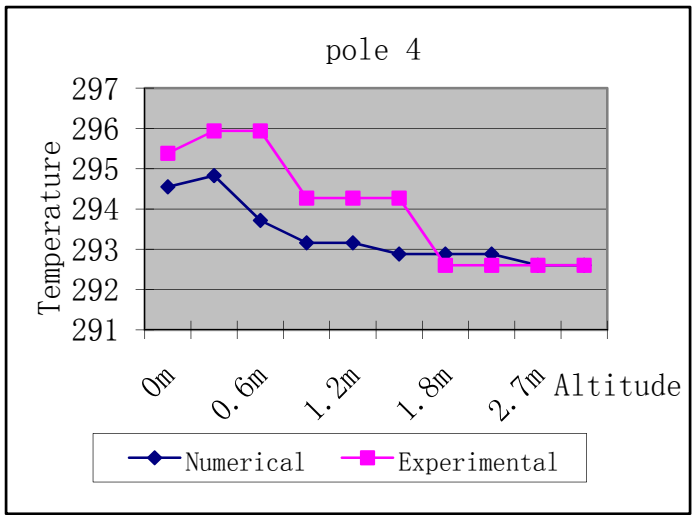

Figure18. Comparison of measured and simulated temperature result on pole 4

Based on the compassion between numerical results and experimental data, it shows that the prediction of the model is acceptable. For pole 1 and 3, the numerical results agree well with the experimental data, and there is an acceptable error for pole 4. For pole 2, the prediction failure may be caused by the simplification in the model and the complicated flow field due to the instability of the server.

Figure 19 presents the distribution of floor level temperature from the experiment data. Figure 20 shows the comparison of floor level temperature between the numerical result and experiment data. The temperature is measured by electrical thermometer from every $2 \times 2in^2$ floor board of the data center.

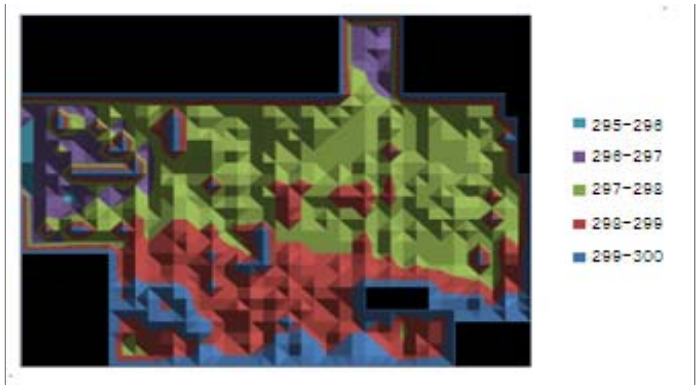

Figure19. Temperature of floor level from the experimental data

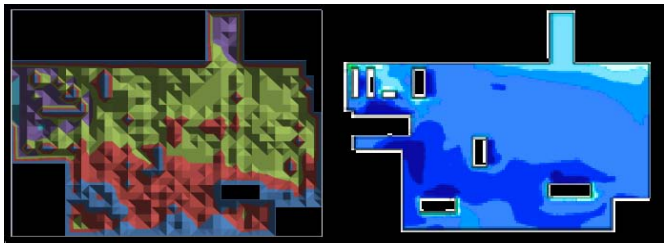

Figure20. Temperature comparison between the numerical result and experimental data

Specific requirement for a data center

The specifications might seem broad for a data center. However, the operating ranges that apply to the absolute hardware limits and the extreme ranges should not be considered guidelines for normal, continuous operation. Therefore, stringent control over temperature, humidity, and airflow is necessary for *optimal* system performance and reliability.

1. Temperature

An ambient temperature range of 294 to 296K (70 to 74 ^{o}F) is optimal for system reliability and operator comfort. A temperature level near 295K (72 ^{o}F) is desirable because it is easier to maintain a safe associated relative humidity level at this temperature. Further, this recommended temperature provides an operational buffer in case the environmental support systems are down.

2. Air Intake Temperatures

Note that the operating temperature range for the servers is either 278 to 313K (41 to 104 ^{o}F) or 278 to 308K (41 to 95 ^{o}F). These temperatures apply to the air taken in by each server at the point where the air enters the server. Ensure that the air intake temperature is within the operating range of the system.

3. Aisle Temperatures

In a hot-aisle/cold-aisle cabinet layout, verify that the temperatures within the cold aisles are also within the servers' operating temperature ranges. These measurements are necessary because temperatures in the data center are different depending on where in the room the measurements are taken. The heat load in the data center can vary as a result of the density of heat-producing equipment located within the room.

4. Humidity

Relative humidity (RH) is the amount of moisture in a given sample of air at a given temperature in relation to the maximum amount of moisture that a sample could contain at the same temperature. A volume of air at a given temperature can hold a certain amount of moisture. Ambient relative humidity levels between 45% and 50% are most suitable for safe server operations. This optimal range also provides the greatest operating time buffer in the event of an environmental control system failure. Data center equipment

is particularly sensitive to high humidity levels. When relative humidity levels are too high, water condensation can occur, which can lead to hardware corrosion problems. Further, maintaining a relative humidity level between 45% and 50% helps avoid system damage or temporary malfunctions caused by intermittent interference from electrostatic discharge, which occurs when relative humidity is too low. Electrostatic discharge is easily generated and less easily dissipated in areas where the relative humidity is below 35%, and becomes critical when relative humidity drops below 30%. Though the 20% to 80% RH operating specifications for the servers are wide, conditions should be maintained near the optimal relative humidity levels which means relative humidity levels are between 45% and 50%. Extremes within the 20% to 80% RH range can lead to unacceptable conditions.

Improvement Suggestions

1. Changing the air flow rate of inlet diffuser

The effect of the inlet air speed on a typical set up was considered in simulations 2, combined with simulation 1 as the basic case. As the inlet air flow rate ranges from 12.2 kg/s to 18.3 kg/s, the average air speed is found linearly dependent and ranges from 0.14 m/s to 0.21 m/s. Figure 21 and 22 present the velocity field and vector on the color background of the velocity magnitude distribution.

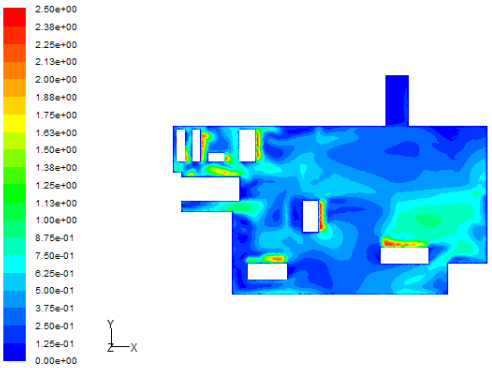

Figure21. Velocity, simulation 2

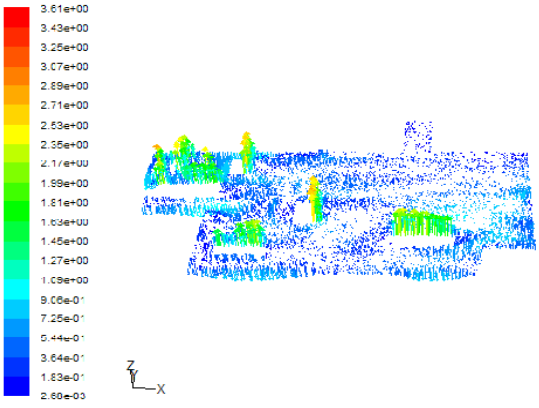

Figure22. Velocity vector

The user defined function (UDF) is used to achieve the purpose of display the difference between two cases in temperature distribution for the analysis of the results. The team uses C programming language to write the codes which can be operated in the software Fluent™. The UDF makes the direct comparing between two different cases possible.

Figure 23-26 show the difference values of the temperature distribution from different altitudes between the improved case and original case.

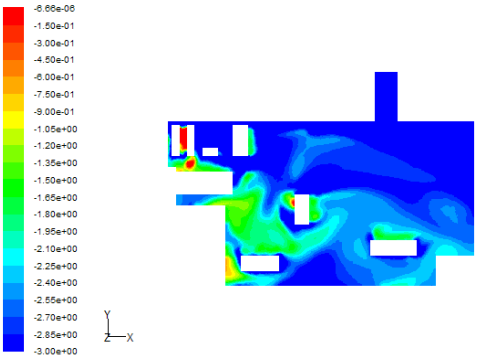

Figure23. The difference values of temperature distribution (altitude 2.0m)

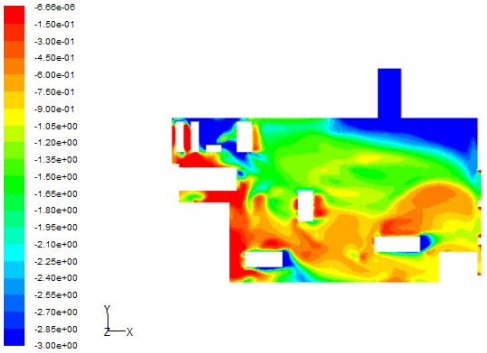

Figure24. The difference values of temperature distribution (altitude 1.5m)

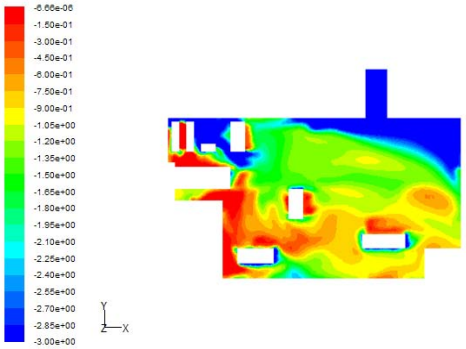

Figure25. The difference values of temperature distribution (altitude 1.0m)

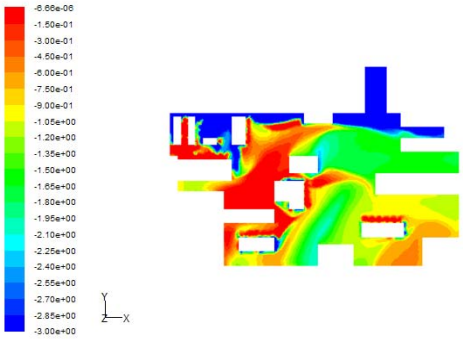

Figure26. The difference values of temperature distribution (altitude 0.0m)

Considering the difference values of temperature distribution, it proves that increasing the air flow rate can improve the air condition system cooling effect. Especially in the danger areas, the temperature of area decrease observably.

2. Changing the amount of water vapor of inlet air flow

Among the simulation 3 with different amount of water vapor of the inlet air flow, it is found that the average temperature is lower than simulation 1. Simulation 3 represents the case with 20% extra relative humidity of the air flow from the inlet, which based on the simulation 1, thus the significantly different flow pattern on Fig. 25 and 26.

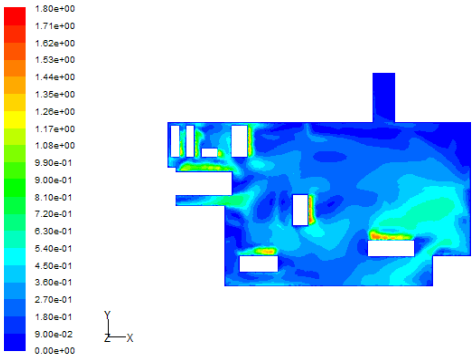

Figure25. Velocity, simulation 3

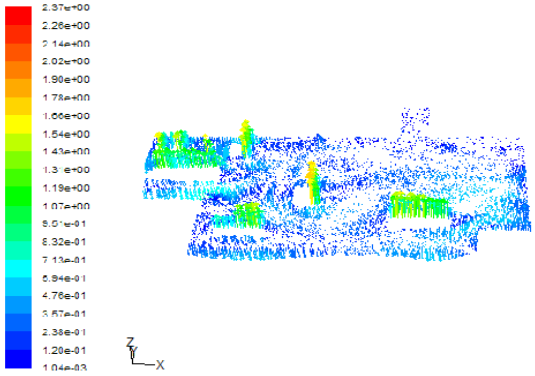

Figure26. Velocity vector

Figure 27-30 show the difference values of the temperature distribution from different altitudes between the improved case and original case. Red color in the magnitude represents the temperature decreasing .about 3K.

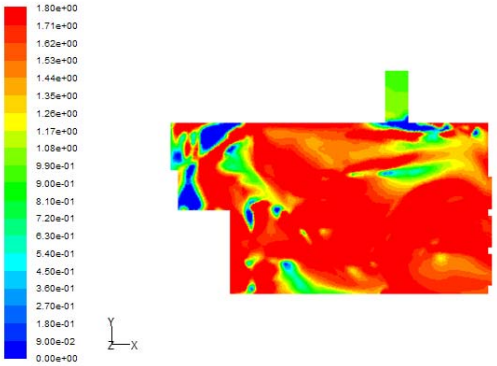

Figure27. The difference values of temperature distribution (altitude 2.0m)

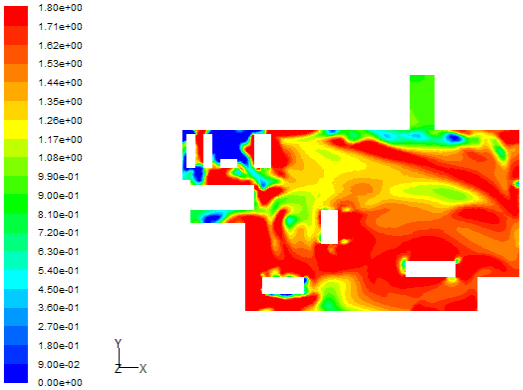

Figure28. The difference values of temperature distribution (altitude 1.5m)

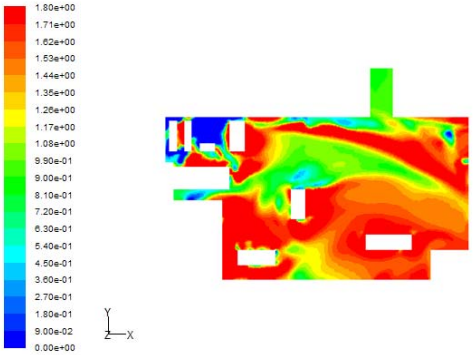

Figure29. The difference values of temperature distribution (altitude 1.0m)

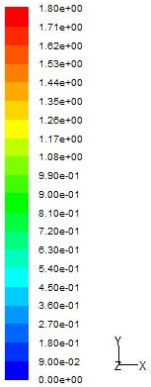

Figure30. The difference values of temperature distribution (altitude 0.0m)

Considering the difference values of temperature distribution, it proves that increasing the amount of water vapor of the air flow can improve the air condition system cooling effect and save the energy consumptions as well.

Comparison of simulation 1 and simulation 3 relative humidity distributions and results are shown in Fig. 31. It proves that the increasing the amount of water vapor of the air flow can reduce the range of the danger areas. The relative humidity levels between 45% and 50% are most suitable for safe server operations of the data center.

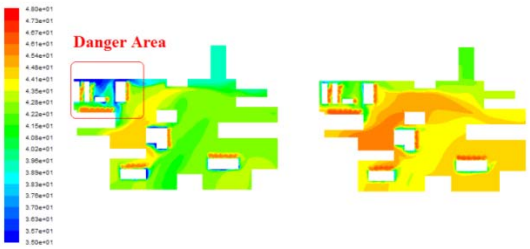

Figure31. Comparison of simulation 1 (left) and simulation 3 (right)

CONCLUSION

1. The simulation results are consistent well with experimental data, which shows the accuracy and reliability of the numerical algorithm and turbulent model in indoor air environments simulation. Results can be used to optimize the design of the air conditional system for the data center.

2. According to the paper, the temperature field in the data center is acceptable. The problem is that the relative humidity level in the dangerous area is too low, which can cause the electrostatic discharge and malfunction. The solution is to increase the amount of water vapor at the inlet thus to keep the relative humidity field within the optimal range.

3. In consideration of the preliminary results, we are testing different possible influence factors for indoor air cooling effects for the data center, such as air flow rate, and different the mass fraction of water vapor of inlet air flow. Research works are going on for this topic.

REFERENCES

1. Woods J.E., "What Real-World Experience Says about UFAD Alternatives," *ASHRAE Journal*, 46 (2), pp. 3-15, 2004.
2. Webster T.W., Bauman F., and Reese J., "Under floor Air Distribution: Thermal Stratification," *ASHRAE Journal*, 44 (5), pp. 28-33, 2002.
3. Stanke D., "Turning Air Distribution Upside Down Under floor Air Distribution," *Engineers Newsletter*, 30 (4), 2001.
4. Wang X. and Pepper D. W., "Numerical Simulation for Under-Floor Air Distribution System with Swirl Diffusers", *ASME Journal of Heat Transfer*, 129, pp. 589-594, 2007.
5. Chow W.F. and Fung W.F., "Numerical Studies on Indoor Air Flow in the Occupied Zone of Ventilated and Air-Conditioned Space," *Building and Environment*, 31, pp. 319-344, 1996.
6. Emmerich S.J., "Use of Computational Fluid Dynamics to Analyze Indoor Air Quality Issues," *NISTIR 5997, Building and Fire Research Laboratory, National Institute of Standards and Technology, Gaithersburg*, MD, 1997.
7. Jelena Srebric, "CFD Boundary Conditions for Contaminant Dispersion, Heat Transfer and Airflow Simulations Around Human Occupants in Indoor environments," *Building and Environment*, 43, 294–303, 2008.
8. ASHRAE, 2001, ASHRAE Handbook of Fundamentals, American Society of Heating, Refrigerating and Air Conditioning Engineers, Inc., Atlanta, Georgia.